Proceedings of the ASME 2012 Summer Bioengineering Conference
SBC2012
June 20-23, Fajardo, Puerto Rico, USA

SBC2012-80557

# TOWARDS A BIOMECHANICALLY-BASED DIAGNOSIS FOR GLAUCOMA: IN VIVO DEFORMATION MAPPING OF THE HUMAN OPTIC NERVE HEAD

**Michaël J.A. Girard (1), Lyn Zimmo (2), Edward T. White (2), Jean Martial Mari (3), C. Ross Ethier (1), and Nicholas G. Strouthidis (2)**

(1) Department of Bioengineering
Imperial College London
London, United Kingdom

(2) NIHR Biomedical Sciences Center
Moorfields Eye Hospital &
UCL Institute of Ophthalmology
London, United Kingdom

(3) INSERM U1032
Université de Lyon
Lyon, France

## INTRODUCTION

Glaucoma is the most common cause of irreversible blindness. It is associated with a progressive loss of cells within the optic nerve head (ONH) at the back of the eye. Glaucoma remains incurable and its exact causes are not well understood. It was once thought to occur only in eyes with elevated pressure (i.e., intraocular pressure or IOP) and to date, lowering IOP is the only clinical treatment proven to be beneficial for slowing the progression of glaucoma. However, the success rate of such therapy is only 50%. Multiple lines of evidence now indicate that IOP is not the only important risk factor in the disease. For instance, while some patients develop glaucoma at elevated IOP (high-tension glaucoma), some develop glaucoma at normal IOP levels (normal-tension glaucoma), and some others with elevated IOP do not develop glaucoma at all.

Our previous research [1], and that of others [2-4], has set out to provide explanations for the above clinical observations, and suggested that the biomechanics of an individual's ONH dictates the IOP level it can safely sustain; above an individual-specific threshold level of IOP, a series of cellular events will be initiated and eventually lead to glaucomatous damage.

We use a combination of state-of-the-art clinical imaging (i.e., optical coherence tomography or OCT) and computational tools to non-invasively measure the in-vivo biomechanical characteristics (strain, stress, mechanical properties) of an individual's ONH. In this study, we report for the first time successful 3D deformation mapping of the human ONH in vivo.

## MATERIAL AND METHODS

### *Clinical Aspects*

Four patients were recruited for this study: 3 high-tension and 1 normal-tension glaucoma patients with pre-operative IOPs of 36, 24, 23, and 14 mmHg, respectively. All underwent glaucoma surgery (trabeculectomy or TE) to reduce the IOP by 24, 13, 6 and 4 mmHg, respectively. Each patient's ONH was non-invasively imaged in 3D using OCT before (< 5 days) and after (< 5 weeks) TE. Each OCT scan of the ONH (496×384×145 voxels) was averaged 9 times during acquisition to reduce speckle noise and thus improve image quality.

### *Computational Aspects*

OCT image quality was further improved by removing blood vessel shadow artifacts and by increasing the visibility of the deepest ONH connective tissues such as the sclera and the lamina cribrosa (LC; Figure 1) [5]. These tissues are biomechanically important, as they are the main load-bearing structures within the ONH.

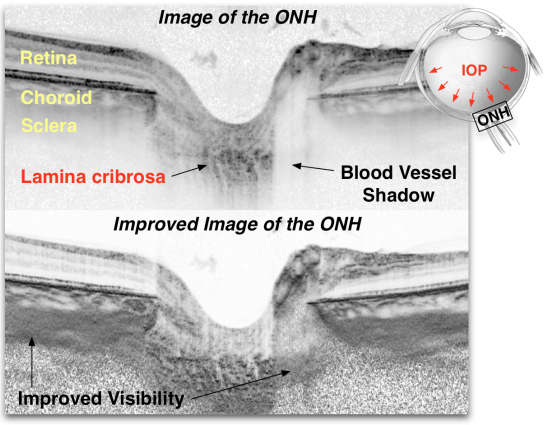


**Figure 1. Quality improvements in OCT images of the ONH.**

Each pre-TE volume was then manually segmented to isolate the following tissue groups: 1) retina and neural tissues; 2) choroid and Bruch's membrane; 3) Sclera; 4) LC (Figure 2). Segmented ONHs were then meshed using 4 node-tetrahedrons containing approximately 7,000 nodes.

An OCT-based 3D tracking algorithm was developed using the principle of digital volume correlation [6] to extract the resulting 3D ONH displacements following TE. Briefly, regions of interest (ROIs) were created in the pre-TE volume by centering a cubing sub-volume (21×21×21 voxels) at each node where a displacement vector was sought. Each ROI was subjected to 4 possible affine transformations (rigid translation, rigid rotation, stretch/compression, and shear) until it best matched a colocalised ROI in the post-TE volume. This optimization step, driven by the differential evolution algorithm [7], allowed to extract an IOP-induced displacement vector for each node.

For each ONH, the 3D displacement field was then filtered to remove physically incoherent vectors, and smoothed using smooth particle hydrodynamics. The Green-Lagrange strain tensor was then computed for each tetrahedron of the mesh.

Our 3D tracking algorithm was validated using artificially deformed volumes of known deformation with a superimposed model for speckle noise. We found that our algorithm was robust to speckle noise and in best conditions could extract displacements with a total error of 0.23 µm and effective strains with a total error of 0.0033.

## RESULTS

Following IOP lowering by glaucoma surgery, we observed contraction of the scleral canal in all 4 patients by 1.23%, 2.55%, 0.65%, and 0.97%, respectively. In all but patient 2, we observed outward movement (mean displacements of 11.3, 5.6 and 3.8 µm, respectively) and thickening (mean compressive strains of -2.66%, -2.29% and -0.08%, respectively) of the LC. Conversely, in patient 2, we observed inward movement (mean displacement of -39.4 µm) and thinning (mean compressive strains of 6.02%) of the LC (Figure 2).

## DISCUSSION

We present here novel engineering tools that can map 3D deformations of the ONH in vivo for the first time. We also demonstrate that ONH displacements and strains are detectable in vivo and that TE can induce contraction of the scleral canal and relieve compressive strains within the LC in almost all patients. Strain relief in the LC (to various degrees) could explain why glaucomatous progression may be slowed following TE. We believe this work is an exciting first step towards the foundation for a novel theory to accurately predict the development and progression of glaucoma.

## REFERENCES


1. Girard, M. J., Suh, J. K., Bottlang, M., Burgoyne, C. F., and Downs, J. C., 2011, "Biomechanical changes in the sclera of monkey eyes exposed to chronic IOP elevations," Invest Ophthalmol Vis Sci, 52(8), pp. 5656-5669.
2. Sigal, I. A., and Ethier, C. R., 2009, "Biomechanics of the optic nerve head," Exp Eye Res, 88(4), pp. 799-807.
3. Yan, D., McPheeters, S., Johnson, G., Utzinger, U., and Vande Geest, J. P., 2011, "Microstructural differences in the human posterior sclera as a function of age and race," Invest Ophthalmol Vis Sci, 52(2), pp. 821-829.
4. Myers, K. M., Cone, F. E., Quigley, H. A., Gelman, S., Pease, M. E., and Nguyen, T. D., 2010, "The in vitro inflation response of mouse sclera," Exp Eye Res, 91(6), pp. 866-875.
5. Girard, M. J., Strouthidis, N. G., Ethier, C. R., and Mari, J. M., 2011, "Shadow removal and contrast enhancement in optical coherence tomography images of the human optic nerve head," Invest Ophthalmol Vis Sci, 52(10), pp. 7738-7748.
6. Bay, B. K., 2008, "Methods and applications of digital volume correlation," The Journal of Strain Analysis for Engineering Design, 43(8), pp. 745-760.
7. Price, K. V., Storn, R. M., and Lampinen, J. A., 2005, Differential evolution. A practical approach to global optimization. , Springer, Berlin, Germany


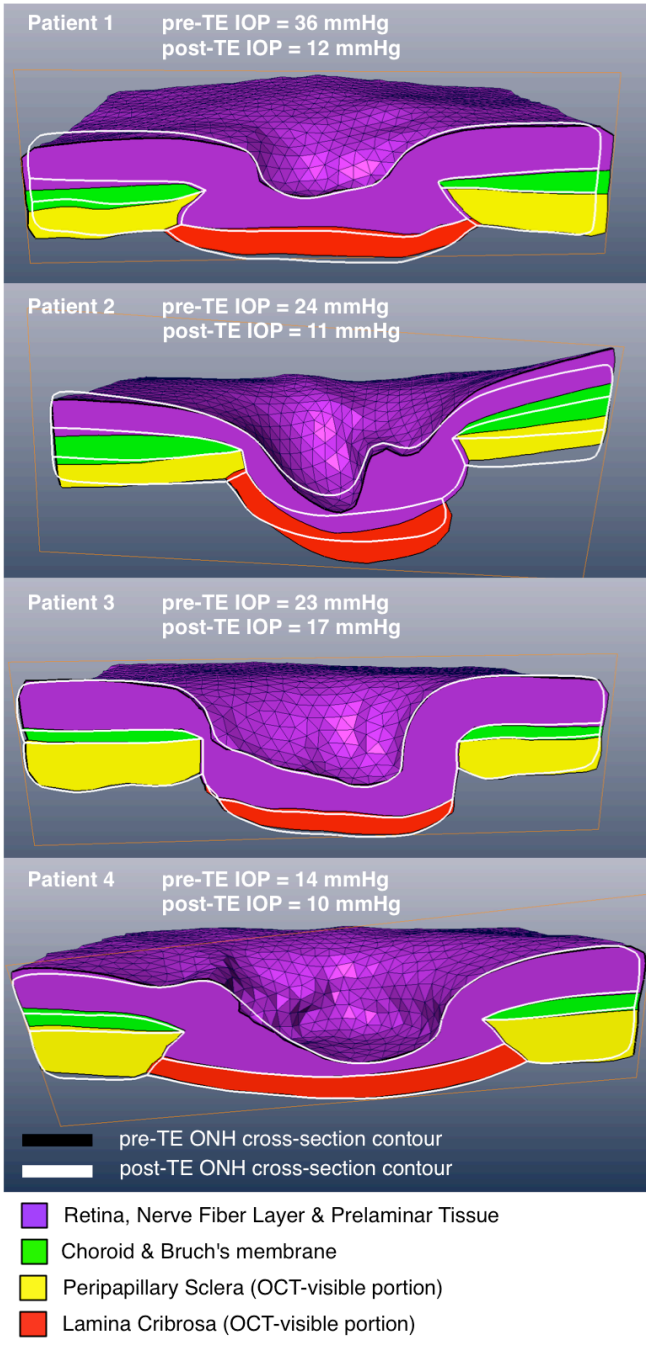


**Figure 2. In vivo 3D deformation mapping of the ONH following TE. Cross-sectional contours of the ONH pre- and post-TE are shown in black and white, respectively. Displacements were exaggerated twofold.**